Physica D 238 (2009) 1827–1840

Contents lists available at ScienceDirect

Physica D

journal homepage: www.elsevier.com/locate/physd

Probing a subcritical instability with an amplitude expansion: An exploration of how far one can get

Paul Becherer [a,*,1], Alexander N. Morozov [b], Wim van Saarloos [a]

[a] Instituut-Lorentz for Theoretical Physics, Universiteit Leiden, Postbus 9506, NL-2300 RA Leiden, The Netherlands

[b] School of Physics, University of Edinburgh, JCMB, King's Buildings, Mayfield Road, Edinburgh EH9 3JZ, United Kingdom

ARTICLE INFO

Article history:
Received 4 July 2008
Received in revised form
15 January 2009
Accepted 19 March 2009
Available online 26 March 2009
Communicated by A. Doelman

PACS:
02.30.Jr
02.30.Mv
05.45.-a
47.20.Ky
47.54.+r

Keywords:
Subcritical instabilities
Amplitude expansion

ABSTRACT

We explore methods to locate subcritical branches of spatially periodic solutions in pattern forming systems with a nonlinear finite-wavelength instability. We do so by means of a direct expansion in the amplitude of the linearly least stable mode about the appropriate reference state which one considers. This is motivated by the observation that for some equations fully nonlinear chaotic dynamics has been found to be organized around periodic solutions that do not simply bifurcate from the basic (laminar) state. We apply the method to two model equations, a subcritical generalization of the Swift–Hohenberg equation and a novel extension of the Kuramoto–Sivashinsky equation that we introduce to illustrate the abovementioned scenario in which weakly chaotic subcritical dynamics is organized around periodic states that bifurcate "from infinity" and that can nevertheless be probed perturbatively. We explore the reliability and robustness of such an expansion, with a particular focus on the use of these methods for determining the existence and approximate properties of finite-amplitude stationary solutions. Such methods obviously are to be used with caution: the expansions are often only asymptotic approximations, and if they converge their radius of convergence may be small. Nevertheless, expansions to higher order in the amplitude can be a useful tool to obtain qualitatively reliable results.

1. Introduction

Many non-equilibrium systems show spatio-temporal instabilities of some kind: ripples on sand, convection rolls in fluids, turbulence in pipe flows, patterns in crystal growth, etc. If they are driven far enough away from equilibrium (usually quantified by some control parameter), a homogeneous initial state (say, a flat bed of sand, a laminar flow or a straight front) becomes unstable with respect to spatial perturbations of a certain wavelength. Often, perturbations with a wavenumber around a critical wavenumber start to grow, and the system ends up in an inhomogeneous state. This state may feature regular stationary or oscillatory patterns, travelling waves, or even spatiotemporal chaos or turbulence. Such *finite-wavelength instabilities* and the patterns they give rise to have been the focus of much research in the past few decades [1–8].

As is well known, there are a number of ways in which the transition from a homogeneous state to a patterned state can occur. Three of the most important ones are depicted schematically in Fig. 1. In (a) we sketch the common *supercritical* transition scenario, in which a stable pattern branch bifurcates off the homogeneous state at the point at which the homogeneous steady state becomes linearly unstable at some critical value of the control parameter. This scenario occurs frequently when the nonlinearities in the system lead to saturation. The amplitude of the pattern vanishes as the control parameter approaches its critical value from above. Close to the transition point, the amplitude generally scales as the square root of the distance to the transition point. A well-known example of this type of transition is the transition to rolls in Rayleigh–Bénard convection [1]. Fig. 1(b) depicts the case of a *subcritical* bifurcation: the system becomes linearly unstable beyond a critical value of the control parameter, but even below this point, there are nontrivial finite amplitude pattern solutions. The amplitude no longer vanishes when the critical point is approached from above. This type of behavior is found for example in Rayleigh–Bénard convection with non-Boussinesq effects [9,5], and in in many other systems without an "up–down" symmetry, like 2-dimensional reaction-diffusion systems with a Turing instability [10,5]. In Fig. 1(c) we finally sketch the case which is sometimes referred to as a *bifurcation from infinity* [11]: the homogeneous state is linearly stable for *all* values of the control parameter, but for sufficiently large control parameters there exists a branch of finite amplitude nontrivial solutions which in

* Corresponding author. Tel.: +31 71 332 2056; fax: +31 71 527 5511.
E-mail addresses: becherer@lorentz.leidenuniv.nl, pbech@dds.nl (P. Becherer).
[1] Present address: Culgi BV, Postbus 252, NL-2300 AG Leiden, The Netherlands.

0167-2789/$ – see front matter © 2009 Published by Elsevier B.V.
doi:10.1016/j.physd.2009.03.009

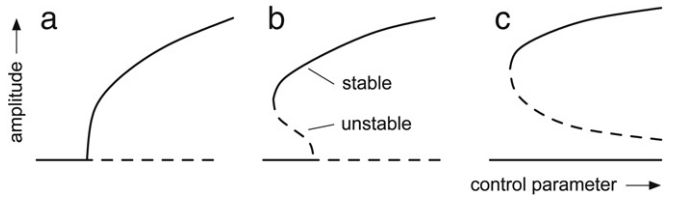

Fig. 1. Typical bifurcation diagrams for (a) a supercritical transition, (b) a subcritical transition and (c) a subcritical bifurcation from infinity. Solid lines denote linearly stable states, dashed lines are linearly unstable. Note that in practice the nonlinear solutions on the upper branch are sometimes not actually stable, but in such cases they can still organize the dynamics. This happens for instance in the transition to turbulence in Couette and pipe flow [12,13] and in the equation we construct and analyse in Section 4.

practice govern the dynamics of the system under some conditions. The lower (unstable) branch defines a kind of threshold amplitude: if perturbations are smaller than this amplitude, the system returns to the homogeneous state; if they are larger, the system ends up on the upper branch. The best known example of this scenario is the transition to turbulence in Newtonian fluids in plane Couette or Poiseuille pipe flow, although the nature of the "stable" and "unstable" branches is not at all clear in this case [12,13]. Two of us recently proposed that the same scenario may apply to shear flows of non-Newtonian viscoelastic fluids [14,15]. Note that while in the figure we indicate the upper branch to consist of stable solutions, this is often not the case in practice. One example is given by the exact two-dimensional nonlinear states in the form of travelling waves that were found in Newtonian plane channel flow [16]. On the upper branch, these solutions are stable in two dimensions, but they are unstable when an infinitesimally small three-dimensional perturbation is introduced [17]. Another example is Newtonian turbulence in pipe flows where three-dimensional nonlinear solutions play an important role in the dynamics, even though they are themselves unstable [12,13].

The partial differential equations that usually describe pattern-forming systems cannot be solved analytically in general. However, as the bifurcation diagrams already suggest, near a transition it is often possible to find a reduced description of the spatially periodic or travelling-wave solutions in terms of just the amplitude of the pattern. For supercritical transitions, the *amplitude equation* approach has been very successful [1–8].

For strongly subcritical transitions, however, this approach essentially breaks down. At the transition, the stable branch already has a nonzero amplitude, and the usual expansion in principle does not work, at least not for the most relevant stable (upper) branch. The lower branch of unstable solutions still grows as in the supercritical case, so unstable states can be found perturbatively sufficiently close to the transition (and thus, threshold amplitudes of perturbations). If the subcritical character is sufficiently weak, it is often possible to adapt the expansion to find also the stable solutions, as for example in Rayleigh–Bénard convection with non-Boussinesq effects [9]. The expansion is then formally no longer consistent, but works in practice because effectively there is a another small parameter (e.g., the smallness of the non-Boussinesq effects).

From a more formal point of view, one might argue that one simply should not use amplitude expansions to probe subcritical bifurcations and especially the bifurcations from infinity of Fig. 1(c) that motivate us, since the amplitude expansion, *which is only an asymptotic expansion*, can clearly not be trusted to give reliable results about the existence and stability of finite-amplitude patterns. In practice, however, such a strict point of view is not the most constructive one. After all, if one is investigating a new problem about which not much is known a priori, one does not necessarily know in advance whether patterns one observes are due to some supercritical or subcritical transition, or even a bifurcation from infinity—one actually does a calculation to find out what the nature of the problem is! Suppose then one finds in an amplitude expansion that the sign of the cubic nonlinearity signals that there is no saturation of the pattern amplitude at the lowest nontrivial level, in other words, that the bifurcation is not supercritical. Should one then simply stop at that point because the amplitude expansion formally cannot handle such a situation?

Clearly, such a defeatist attitude is not to be expected from an applied researcher who is eager to understand the nonlinear behavior of the problem at hand. In practice, if there is reason to believe on physical grounds that the transition is weakly subcritical, even though there may be no a priori small parameter in the equations that suggests this, such a practitioner of nonlinear science may want to try, nevertheless, to calculate the next (fifth order) term in the expansion, in the hope of being able to estimate how weak the subcritical character really is, and how large the amplitudes of the nonlinear pattern actually might be. And if such a calculation is done, one faces the question as to how reliable this estimate actually is and what the optimal truncation (if any) of the expansion might be.

Two of us recently faced a similar dilemma in a study of the nonlinear stability of viscoelastic shear flows [14,15,18] where we suspected, on physical grounds, the relevance of the bifurcation from infinity scenario of Fig. 1(c). Motivated by the expectation that the lower (unstable) branch – which determines the nonlinear instability threshold – would actually be close to the horizontal axis for intermediate values of the control parameter, and that the smallness of the transition amplitude could play the role of an intrinsic small parameter hidden in the problem, an amplitude expansion up to eleventh order was performed to estimate the nonlinear threshold. In this case, it actually does appear that useful information can be extracted from analyzing the behavior of the expansion to such high orders.

This paper is motivated by these observations and by our own experience, that even though hard and generally valid statements are difficult to make about the behavior of intrinsically asymptotic expansions, it is very profitable to get a better feel for how far one may push amplitude expansions to probe such intrinsically subcritical transitions. One of the main aims of this paper is to explore the possible signatures for failure or success of this pragmatic approach. Indeed, in studying these issues, we have empirically found that it is sometimes possible to push the expansions further by focusing on a limited question, like the existence and nature of a nonlinear (subcritical) branch of solutions. We discuss this method and its basis, and compare it to the results one obtains from a more straightforward amplitude expansion. Moreover, in order to illustrate that such expansion methods can even be useful in cases in which the nonlinear solutions that one can probe perturbatively are unstable but nevertheless important for the dynamics, we introduce a new simple model based on two coupled equations whose bifurcation diagram corresponds to the "bifurcation from infinity" case of Fig. 1(c), and which mimics a case in which Kuramoto–Sivashinsky-like chaos [19–21] is organized around exact periodic solutions. The gross features of the turbulent nonlinear branch of this equation are indeed captured well with our amplitude expansion, a finding that gives hope for our earlier work on nonlinear visco-elastic instabilities [15].

We stress here at the outset that our goal is rather limited. First of all, the equations we study are only used as exploratory examples. Secondly, we *neither* aim *nor* claim to investigate the full nonlinear dynamics of these equations; instead, we will focus simply on determining the presence and location of the subcritical branches of periodic solutions in the approximation so that only the amplitude of one mode is retained. The stability of the branches is hence only studied within this subspace of periodic solutions

that are identified by a single amplitude. Clearly, these solutions may well be unstable in other directions in function space, so whether such results have anything to do with the full nonlinear dynamics of any equation under study cannot be settled without additional (often numerical) studies. Our discussion in Section 4 of the chaotic dynamics in the coupled Kuramoto–Sivashinsky-like model equation will illustrate this.

To help the reader better understand our motivation, we recall again the transition to turbulence scenario in plane Couette or plane and pipe Poiseuille flow of Newtonian fluids [12,13]. For these cases it has become clear in recent years that the Navier-Stokes equations admit exact periodic solutions [22–24] which do not bifurcate off the laminar state. Even though these solutions themselves are weakly unstable in nontrivial directions, the turbulent dynamics is organized around these exact nonlinear periodic traveling wave states (through a so-called Self-Sustaining Process [13,25] in which the instability eventually pumps energy back via vortices into traveling wave modes). Probing the existence of these solutions is clearly a first step in such an analysis. Moreover, as recent work on turbulent Poiseuille flow illustrates, once such solutions have been found, they can sometimes be traced with continuation methods[2] by introducing an additional driving term in the equations. But when such solutions do not bifurcate in a simple way off the base state (the laminar flow state), or when they emerge via a "bifurcation from infinity", the amplitude methods we explore here may be a useful first step. That this is not just a dream is indeed illustrated by the model equation we introduce in Section 4: this equation is constructed so as to have subcritical branches of periodic solutions that conform to the bifurcation from infinity scenario. We find that these solutions can be located reasonably accurately by the two expansion methods we introduce. Moreover, numerical simulations confirm that the chaotic dynamics is, in a well-defined way, organized around these branches of periodic solutions — the model equation is thus a simple caricature of the transition to turbulence scenario in Couette and Poiseuille flow [12,13].

In summary, then, the main goals of the paper are (i) to investigate the performance of amplitude expansions in higher orders by exploring the signals for when the results can or cannot be trusted; (ii) to demonstrate that besides the usual amplitude expansion method, there is a second, more restricted expansion method which focuses immediately on stationary manifolds. We show that in the examples we consider, this method II appears to have a finite range of convergence, and we propose an intuitive understanding of this and of the difference with the regular expansion method. (iii) to illustrate, with the Kuramoto–Sivanshinsky-like model we introduce, that the expansion methods can be of use to approximately locate the chaotic dynamics around branches that bifurcate off infinity.

Both methods we employ in this paper are variants of the usual amplitude expansion, aimed in particular at studying the stability and approximate dynamics of a spatially extended system with a subcritical finite-wavelength instability. We derive a single ordinary differential equation that should capture the essential qualitative features of the transition. The method relies on a direct expansion in the amplitude of the relevant solutions, rather than in the distance to the bifurcation point. There is some freedom in the implementation of this idea, and we actually give two distinct but related versions of the method. Though one of them is based on the standard amplitude expansion approach and though elements of the second approach have appeared in other fields [26,27], a comparison of the two has, to our knowledge, not appeared from the perspective presented here.

The concepts underlying such amplitude expansions are fairly general, and they occur in very diverse fields of pure and applied science. In fact, the use of such amplitude expansions has a long history in fluid mechanics. It was pioneered by Landau [28], Stuart [29] and Watson [30], who used such expansions to describe the subcritical modes in plane Poiseuille flow below the linear instability threshold of Re $\approx$ 5772. This approach was later explored to high order[3] by Herbert [31]. A well-known early monograph on the subject of nonlinear stability theory, including amplitude expansions, was written by Eckhaus [32]. The field of what we now usually properly call amplitude equations started with the seminal work of Newell and Whitehead [33], who included slow spatial modulations in their equations. We will say more about the connections with previous work in other fields further on in this paper. Here we will just mention that since we expand in the amplitude itself rather than the small growth rate, our method resembles most closely that of Watson [30], although formal equivalence between several possible methods has been established [34–36].

As in these earlier approaches, we will focus in this paper on expansions in the mode amplitude of periodic patterns with a given wavelength. There are two reasons for this: the first pragmatic reason is that we do not want to overly complicate the analysis. The second, more fundamental reason is that there is no reason to expect that the slow spatial variation of the amplitude and wavelength of a pattern, which is such a characteristic feature of the pattern dynamics just above a supercritical bifurcation, extends to subcritical patterns—if the complex dynamics of a pattern forming or chaotic or turbulent problem is organized around a branch of nonlinear periodic solutions, slow spatial modulations of these solutions is typically not one of the dominant characteristic features of the dynamics. Nevertheless, it will be of interest to extend the analysis to include two or three basis modes—this may in fact extend the range of applicability of the expansion for the subcritical Swift–Hohenberg equation, as we shall see.

A final word about nomenclature: although the word "mode expansion" is sometimes favored over amplitude expansion for approaches like ours where the spatial modulation of the patterns is not studied, we will use the word mode expansion and amplitude expansion interchangeably here.

The outline of this paper is as follows. We will first give in Section 2 a general description of the amplitude expansion and then apply it to two model equations. The first, discussed in Section 3, is a modification of the well-known Swift–Hohenberg model for pattern formation [37,1]. This partial differential equation is one of the simplest pattern-forming systems, and it is modified so that it shows subcritical behavior instead of the usual supercritical transition [38,39,5,40]. The second application, studied in Section 4, is the extended Kuramoto–Sivashinsky-like equation that we introduce to explore a "bifurcation from infinity" transition to weak chaos. In both cases we compare the results of the expansion for periodic solutions with direct numerical simulations of the full partial differential equations, and explore the applicability and limitations of the expansion method.

[2] Of course, once the existence and rough location of periodic solutions is known, continuation methods will yield more accurate results regarding their properties. Expansion methods may be especially of help if one is initially in the dark as to where to look [23,24] but expects their existence on physical grounds. Moreover, for nontrivial problems, continuation methods may easily translate into of order 10^5–10^6 coupled equations. Although problems of this size can nowadays be handled numerically, the conceptual simplicity of an expansion and the fact that it translates into a few coefficients may give additional insight. Both methods have their advantages and disadvantages.

[3] It is useful to point out here that the 3D nonlinear traveling wave states that organize the turbulent dynamics are *not* the 2D states studied by Herbert [31]. Indeed, the former periodic states exist for Couette and pipe Poiseuille flow as well, even though there is no linear instability there, as the scenario corresponds to the "bifurcation from infinity" of Fig. 1(c).

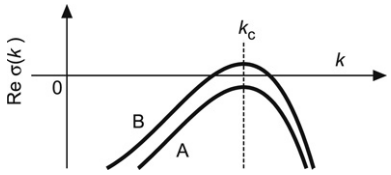

Fig. 2. Linear growth rate $\mathrm{Re}\,\sigma(k)$ as a function of wavenumber k for systems with a finite-wavelength instability, slightly below (A) and above (B) the onset of this instability.

2. Amplitude expansion scheme

In many pattern-forming systems, such as Rayleigh–Bénard convection or Couette flow, one has to consider the spatial dependence in both the translation-invariant direction and the orthogonal (confined) direction. In this paper we shall not deal with this complication, and we shall concentrate on models with one (translation-invariant) spatial dimension. For future reference in our discussion of the mode expansion, we first briefly summarize the general formal setting of the type of problems we will analyze.

We consider $(1+1)$-dimensional PDEs of the form

$$\frac{\partial u}{\partial t} = \hat{\mathcal{L}}\, u + f\left(u, \frac{\partial u}{\partial x}, \frac{\partial^2 u}{\partial x^2}, \dots\right), \tag{1}$$

where $u(x,t)$ is real. The linear operator $\hat{\mathcal{L}}$ contains spatial derivatives; the nonlinear part $f(\cdot)$ is a function of u and its spatial derivatives. We assume that f is a polynomial consisting of only a few terms, with no constant term, so that the PDE always has a trivial solution $u \equiv 0$. This solution corresponds to the homogeneous state in a pattern-forming system. We assume that the linear operator $\hat{\mathcal{L}}$ and the boundary conditions are such that the eigenfunctions of $\hat{\mathcal{L}}$ are plane waves of the form $\mathrm{e}^{\mathrm{i}kx}$, with k real, as is usually the case for translation-invariant systems.

Linear stability analysis around the trivial solution is then straightforward. Insert the *Ansatz*

$$u(x,t) = A\,\mathrm{e}^{\sigma t}\mathrm{e}^{\mathrm{i}kx} \tag{2}$$

into the linearized PDE

$$\frac{\partial u}{\partial t} = \hat{\mathcal{L}}\, u, \tag{3}$$

and solve for σ as a function of k. This gives the (linear) dispersion relation $\sigma(k)$. The real part $\mathrm{Re}\,\sigma(k)$ is the linear growth rate of the eigenmode with wavenumber k. We assume that the system is near a finite-wavelength instability. We will quantify this later, but for now, assume that $\sigma(k)$ looks roughly as in Fig. 2, where k_c is the wavenumber for which the growth rate is maximal. The dynamics of the system is then dominated (in a sense that will be specified later) by the modes with wavenumber close to k_c; in a mode expansion one can derive a single differential equation for the amplitude of one of these modes. We can just take a k close to k_c and claim that it is the dominant mode, for example because that is the wavenumber of the finite-amplitude perturbation that we are interested in. Usually, we shall take $k = k_c$ because that is the least stable mode. The 'standard' amplitude equation performs such a reduction, but as mentioned, only works for supercritical transitions.

The goal of our expansion is to obtain a reduced description of the dynamics of the full system near a finite-wavelength instability (either supercritical or subcritical), as a single ODE for the amplitude A of the dominant mode:

$$\frac{\mathrm{d}A}{\mathrm{d}t} = \epsilon A + C_3 A^3 + C_5 A^5 + \cdots. \tag{4}$$

The parameter ϵ determines the linear stability of the trivial solution, the nonlinear terms form a (truncated) power series in A.

2.1. Expansion method

To derive an equation of the type (4), we first perform a Galerkin-type expansion to convert the PDE (1) to a system of ODEs. This is done by expanding the solution of the PDE in a discrete set of orthonormal spatial basis functions with time-dependent coefficients. As basis functions we will choose the eigenfunctions $\mathrm{e}^{\mathrm{i}kx}$ of $\hat{\mathcal{L}}$. Having chosen the basic wavenumber k of the periodic solution that we wish to probe, we concentrate on solutions that consist of this mode *plus* modes that can be generated from it through the nonlinearity. Thus, we expand the solutions of the PDE as

$$u(x,t) \approx \sum_{n=-\infty}^{+\infty} U_n(t)\exp[\mathrm{i}nkx]. \tag{5}$$

Because u is real, we have that $U_{-n}(t) = U_n^*(t)$, where the star denotes complex conjugation. As we already mentioned, unlike for the supercritical case, for the subcritical case it is not a priori clear which band of wavenumbers we should expect. In fact, the expansion itself will typically be used to probe the range of wavenumbers over which the nonlinear solutions exist, and as long as we disregard explicit spatial modulations or secondary instabilities (for example, side-band or Eckhaus instabilities [32]), we can get away with a mode expansion (5).

The above *Ansatz* is inserted into the full PDE (1), and the result is projected onto the different modes. This gives an ordinary differential equation for each mode. To give an example: suppose that Eq. (1) has a simple quadratic nonlinearity $f(u) = u^2$. The ODE for a particular mode, using the expansion (5), then is

$$\frac{\mathrm{d}U_n}{\mathrm{d}t} = \sigma_n U_n(t) + \sum_{i+j=n} U_i(t)\,U_j(t), \tag{6}$$

where we labeled the eigenvalues of $\hat{\mathcal{L}}$ as $\sigma_n := \sigma(nk)$, and the sum runs over all i and j for which $i+j=n$. Once such a system is obtained, the standard Galerkin procedure is to assume (or show) that only the lowest few modes are relevant, and to restrict the system to these modes, obtaining an approximate description of a partial differential equation in terms of a low-dimensional system of ordinary differential equations. Since our goal is to obtain a *single* ODE for an amplitude that characterizes the main features of the periodic pattern, we take a slightly different approach.

To reduce this system to a single equation we assume that (i) the dominant mode, and the modes that it can generate through nonlinear interactions, are the only relevant modes, and that (ii) amplitude and phase of the "generated" modes are at any time completely determined by amplitude and phase of the dominant mode. In the supercritical case, this is due to the fact that higher order mode adiabatically follow ("are slaved to" [41]) the dominant mode for $\epsilon \ll 1$. This is simply due to the separation of time scales between the dominant mode and the other modes, as the dominant mode evolves on a much slower time scale than the quickly decaying slaved modes, that is, $|\mathrm{Re}\,\sigma(\pm k)| \ll |\mathrm{Re}\,\sigma(nk)|$ for $n \neq \pm 1$. We will clarify this assertion in more detail in the next subsection, where we give a more geometrical interpretation of this phenomenon. To emphasize the distinction between dominant and slaved modes, we slightly change notation and write the expansion (5) as

$$u(x,t) = \phi(t)\mathrm{e}^{\mathrm{i}kx} + \phi^*(t)\mathrm{e}^{-\mathrm{i}kx} + U_0(t) + \sum_{n=2}^{\infty}\left[U_n(t)\mathrm{e}^{\mathrm{i}nkx} + U_{-n}(t)\mathrm{e}^{-\mathrm{i}nkx}\right]. \tag{7}$$

We now assume that the U_n can be written as functions of ϕ, and to implement this, we write the U_n as a power series in ϕ. Note that the coefficients U_n that govern the $\mathrm{e}^{\mathrm{i}nkx}$ mode amplitude can

only be generated by terms of order at least $O(\phi^{|n|})$, so U_n should be $O(\phi^{|n|})$ (but $U_0 = O(\phi^2)$!). This leads to the expansion

$$\begin{aligned} U_0(t) &\equiv U_0(\phi) := u_0^{(2)}|\phi|^2 + u_0^{(4)}|\phi|^4 + u_0^{(6)}|\phi|^6 + \cdots \\ U_2(t) &\equiv U_2(\phi) := u_2^{(2)}\phi^2 + u_2^{(4)}|\phi|^2\phi^2 + \cdots \\ U_3(t) &\equiv U_3(\phi) := u_3^{(3)}\phi^3 + u_3^{(5)}|\phi|^2\phi^3 + \cdots \\ &\vdots \end{aligned} \tag{8}$$

The $u_i^{(j)}$ are unknown complex coefficients. The constraint that $u(x, t)$ is real imposes that $u_{-i}^{(j)} = u_i^{(j)*}$. Note that terms with $u_0^{(3)}$, $u_3^{(4)}$, etc. are absent. Also, no higher-order corrections to the fundamental mode are present: all information on the fundamental mode is in $\phi(t)$. This is in contrast with some other approaches, e.g., the one of Herbert [31].

All nonlinear terms in the expansion of the full PDE can now be expanded in powers of ϕ. For the ODE that governs $\phi(t)$, we can expand the right-hand side and collect powers in ϕ. That equation then becomes

$$\frac{\mathrm{d}\phi}{\mathrm{d}t} = \sigma(k_c)\phi + C_3|\phi|^2\phi + C_5|\phi|^4\phi + C_7|\phi|^6\phi + \cdots, \tag{9}$$

where the unknown coefficients C_i depend on the $u_m^{(n)}$. This is the central equation of our approach that plays the role of an effective amplitude equation for the periodic pattern. The main effort in practice will be to calculate the coefficients C_i.

The right-hand side of the equations for the U_n can also be expanded. These equations can then be converted into algebraic equations in two different ways by dealing with the $\mathrm{d}U_n/\mathrm{d}t$. We shall give these methods the rather undescriptive names of *Method I* and *Method II*, because the ideas behind them are rather general, and they go by different names in different fields.

- *Method I* — We can consistently implement the assumption that the U_n are functions of ϕ by inserting their power series expansions into $\mathrm{d}U_n/\mathrm{d}t$ and applying the chain rule. The $\mathrm{d}\phi/\mathrm{d}t$ that are then left over, can be replaced self-consistently with the amplitude equation (9). We are left with algebraic equations in ϕ for each of the U_n, which can be solved order by order in ϕ, to obtain the coefficients C_i. The consistent way in which we expand ensures that within the convergence domain of this expansion, we approximate a curve (or more generally a manifold) defined by the functions $U_n(\phi)$, that is a trajectory of the infinite-dimensional Galerkin ODE system. If the initial condition is on this curve, the system will stay on this *invariant manifold*. This method is related to the *inertial manifold* method of Foias, Sell and Temam [42], Poincaré–Dulac normal forms [43] and centre manifold methods [44].
- *Method II* — We can also follow a different procedure, which is often used for finite-dimensional systems of ODEs with slaving. This procedure is called *adiabatic elimination* by Haken [41] and is essentially the same as what is known in, *e.g.*, chemical kinetics as the *quasi-steady state assumption* [26,27]. It is also strongly connected with ideas from singular perturbation theory [45,46]. We explicitly use the fact that one mode varies much slower than the other modes, and make a distinction between fast, slaved modes and slow, dominant modes. The idea is that in the timescale of the fast modes, the amplitude of the slow mode(s) is essentially constant. This means that on some timescale shorter than that of the slow mode, the fast modes converge to a fixed point ($\mathrm{d}U_n/\mathrm{d}t = 0$) that is determined by the amplitude of the slow mode. There is thus a kind of quasi-steady state, which adiabatically follows the slow mode and is completely determined by the amplitude of that mode. We can then find $U_n(\phi)$ by putting $\mathrm{d}U_n/\mathrm{d}t = 0$ to obtain algebraic equations in ϕ. These can also be solved order by order in ϕ, in general giving different values for the C_i than Method I.

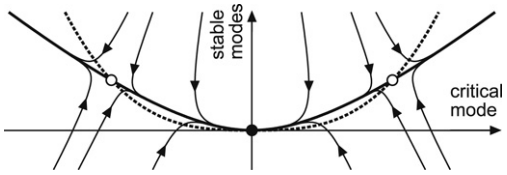

Fig. 3. Generic representation of a dynamical system near a subcritical bifurcation. The horizontal axis represents the amplitude of the critical mode, while the stable modes are lumped together and represented in the vertical direction. The solid dot at the origin represents a stable stationary solution, while the open circles denote unstable ones. The separation between the slow manifold and "horizontal" nullcline, drawn as a dashed line, has been exaggerated for clarity.

2.2. Geometrical interpretation of the methods

To clarify what is going on and to show the difference between the two methods, we give a geometrical picture. In a two-dimensional representation, where the x direction represents the (near-) critical mode and the y direction all stable, slaved modes, the types of systems that we consider look generically as in Fig. 3: the system first evolves quickly towards some type of *slow manifold*, indicated in the figure as the thick line, and the dynamics of the system is effectively determined by the dynamics on that manifold (which can contain fixed points).

The two methods both aim to approximate the slow manifold. Method I does that by demanding that the $U_n(\phi)$ approximate an actual flowline of the effective infinite-dimensional system (6) and thus attempts to approximate the "true" slow manifold. Method II puts $\mathrm{d}U_n/\mathrm{d}t = 0$ for $n \neq 1$, and thus approximates the nullcline where flowlines are horizontal, which is indicated in the figure as a dashed line. This line is not itself a flowline of the system, but lies close to it and contains all fixed points connected to the origin. This geometrical picture will be useful when we analyse the merits of both methods in Section 5.

Note that in practice, the main goal of a perturbative mode expansion is often to indicate the existence and main properties of stationary or travelling wave periodic patterns. In such a case, one is interested in the existence of a fixed point on the slow manifold. The above discussion shows that in principle both methods can be used to try to locate such a fixed point. In practice, however, one method may give more reliable results than the other—establishing whether this is true and under what conditions is one of the main aims of this paper.

3. Generalized Swift–Hohenberg equation

3.1. Description of the model

One of the simplest equations that describes pattern formation is the Swift–Hohenberg model [37,47,48]. It can be viewed as a near-threshold approximation for Rayleigh–Bénard convection [37], but it is usually considered as a simple model in its own right. As such, it has also received attention in the mathematics community, in particular with regard to nontrivial stationary solutions [49,50]. In one spatial dimension it is given by the following fourth-order partial differential equation:

$$\frac{\partial u}{\partial t} = -\left(\frac{\partial^4 u}{\partial x^4} + 2k_c^2\frac{\partial^2 u}{\partial x^2} + k_c^4 u\right) + \epsilon u + c\,u^3, \tag{10}$$

with u, k_c and ϵ real and $c < 0$. This equation always has the trivial solution $u \equiv 0$. It has the form of Eq. (1), with

$$\hat{\mathcal{L}}\,u \equiv -\left(\frac{\partial^4 u}{\partial x^4} + 2k_c^2\frac{\partial^2 u}{\partial x^2} + k_c^4 u\right) + \epsilon\,u \tag{11}$$

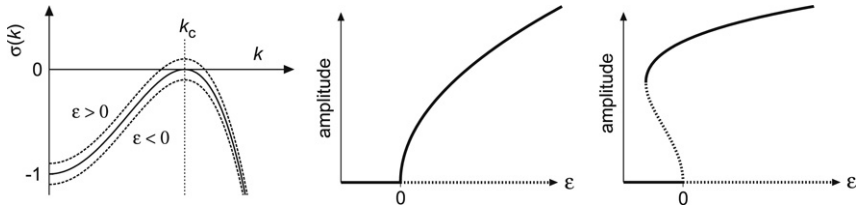

Fig. 4. Linear dispersion relation (a) for original and extended Swift–Hohenberg equations, and corresponding bifurcation diagrams for the original (b) and subcritical (c) Swift–Hohenberg equation.

and

$$f(u) \equiv c\, u^3. \tag{12}$$

It is easy to see that after linearization around the trivial solution, the eigenfunctions of the linear part $\hat{\mathcal{L}}\, u$ are plane waves e^{ikx}, with eigenvalues $\sigma(k) = \epsilon - (k^2 - k_c^2)^2$, see Fig. 4(a); a transition takes place for $\epsilon = 0$, where the eigenvalue for the wave with wavenumber $k = k_c$ becomes positive. Without loss of generality, we can rescale the equation such that $k_c = 1$ and $c = -1$, giving

$$\frac{\partial u}{\partial t} = -\left(\frac{\partial^4 u}{\partial x^4} + 2\frac{\partial^2 u}{\partial x^2} + u\right) + \epsilon\, u - u^3. \tag{13}$$

With the usual amplitude equation approach, the Swift–Hohenberg equation can be reduced to the so-called real Ginzburg–Landau equation (RGLE) [1], which reads, in rescaled form, $\partial_t A = 4\partial_x^2 A + \epsilon\, A - |A|^2 A$ with $A \in \mathbb{C}$.

It is possible to extend the Swift–Hohenberg equation so that it shows subcritical behavior, by adding a term quadratic in the field u [38,39,5,40]:

$$\frac{\partial u}{\partial t} = -\left(\frac{\partial^4 u}{\partial x^4} + 2k_c^2\frac{\partial^2 u}{\partial x^2} + k_c^4\, u\right) + \epsilon\, u + b\, u^2 + c\, u^3, \tag{14}$$

where b is real. The linear stability of the trivial solution is the same as for the original Swift–Hohenberg equation, but the nonlinear behavior is different. In particular, when $b^2/c > 27/38$ (and $c < 0$), the transition at $\epsilon = 0$ becomes subcritical [40], and we have the bifurcation diagram of Fig. 4 (c).

3.2. Amplitude expansion

We are now ready to apply the formalism of Section 2.1 to the extended Swift–Hohenberg equation (14). For convenience we shall rescale the equation such that $k_c = 1$, and we define:

$$\sigma_n \equiv \epsilon - (n^2 k^2 - 1)^2. \tag{15}$$

such that for the eigenfunctions of the linear part we have

$$\hat{\mathcal{L}}\,(e^{inkx}) = \sigma_n\, e^{inkx}. \tag{16}$$

Because the expressions we get upon inserting Eq. (7) into (14) rapidly become cumbersome, we shall write out the terms explicitly only up to third order in the amplitude, and suppress, in our notation, the explicit time-dependence of the amplitudes. Doing this, and remembering that $U_{-n} = U_n^*$, we obtain, after projecting onto the modes nk,

$$\frac{d\phi}{dt} = \sigma_1\,\phi + b\,(2\phi U_0 + 2\phi^* U_2 + \cdots) + c\,(3|\phi|^2\phi + \cdots), \tag{17a}$$

$$\frac{dU_0}{dt} = \sigma_0\, U_0 + b\,(2|\phi|^2 + \cdots) + \cdots, \tag{17b}$$

$$\frac{dU_2}{dt} = \sigma_2\, U_2 + b\,(\phi^2 + \cdots) + \cdots, \tag{17c}$$

$$\frac{dU_3}{dt} = \sigma_3\, U_3 + b\,(2\phi U_2 + \cdots) + c\,(\phi^3 + \cdots), \tag{17d}$$

where the dots represent higher order terms, $O(\phi^4)$. The equations for the other modes contain only terms of order ϕ^4 and higher. We now have a type of Galerkin approximation. The next step is to substitute Eq. (8) into the equation for ϕ. We then obtain

$$\frac{d\phi}{dt} = \sigma_1\phi + b\left[2\phi(u_0^{(2)}|\phi|^2 + \cdots) + 2\phi^*(u_2^{(2)}\phi^2 + \cdots) + \cdots\right] + c\left[3|\phi|^2\phi + \cdots\right]. \tag{18}$$

By collecting the linear and cubic terms, we find an equation of the form (9),

$$\frac{d\phi}{dt} = \sigma_1\phi + C_3|\phi|^2\phi + \cdots, \tag{19}$$

with

$$C_3 = 2b\left(u_0^{(2)} + u_2^{(2)}\right) + 3c. \tag{20}$$

It is now possible to calculate the coefficients $u_i^{(j)}$ by looking at the equations for the U_i. We find, again up to and including $O(\phi^3)$,

$$\frac{dU_0}{dt} = (\sigma_0 u_0^{(2)} + 2b)|\phi|^2 + \cdots, \tag{21a}$$

$$\frac{dU_2}{dt} = (\sigma_2 u_2^{(2)} + b)\phi^2 + \cdots, \tag{21b}$$

$$\frac{dU_3}{dt} = (\sigma_3 u_3^{(3)} + 2b u_2^{(2)} + c)\phi^3 + \cdots. \tag{21c}$$

Note that we have included here the coefficient $u_3^{(3)}$, even though it is not strictly necessary for determining C_3; this coefficient is important for the dynamics of the U_3 mode.

It is now possible to determine the coefficients $u_i^{(j)}$ if we deal with the dU_i/dt in one of the proposed ways. Since from here on the results depend on which expansion method is used, we treat the two methods separately.

Method I. If we use Method I, we find

$$\frac{dU_0}{dt} = \frac{d}{dt}\left(u_0^{(2)}|\phi|^2 + \cdots\right) = u_0^{(2)}\left(\phi\frac{d\phi^*}{dt} + \phi^*\frac{d\phi}{dt}\right) + \cdots, \tag{22}$$

which, upon inserting Eq. (19), becomes

$$\frac{dU_0}{dt} = 2u_0^{(2)}(\sigma_1|\phi|^2 + \cdots) + \cdots. \tag{23}$$

Analogously, we find for the other modes

$$\frac{dU_2}{dt} = 2u_2^{(2)}(\sigma_1\phi^2 + \cdots) + \cdots, \tag{24a}$$

$$\frac{dU_3}{dt} = 3u_3^{(3)}(\sigma_1\phi^3 + \cdots) + \cdots. \tag{24b}$$

We can then begin to separate each equation for the U_i in orders of ϕ. Since these equations are supposed to hold for arbitrary ϕ, they should be satisfied for all orders of ϕ separately. In this particular example we only display terms up to third order, and we find only one order of ϕ for each equation, but to higher order we find

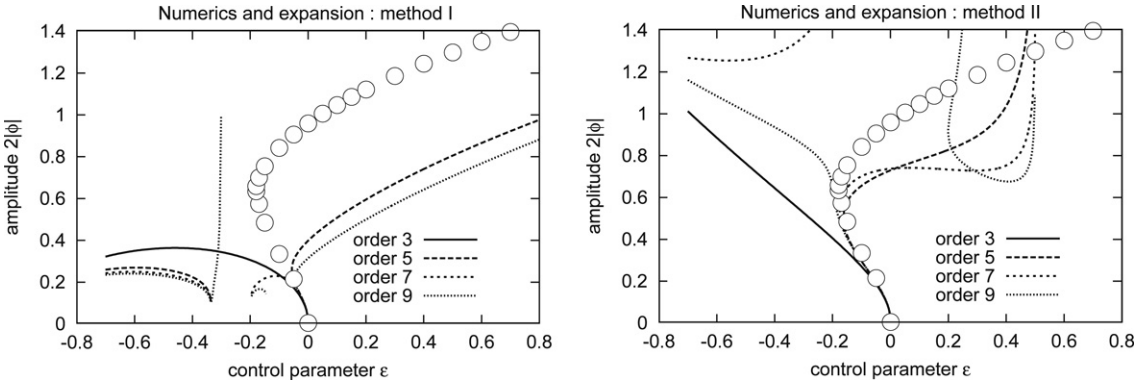

Fig. 5. Comparison between amplitude expansion and numerical solutions for stationary solutions of the extended Swift–Hohenberg equation, for $c = -1.0$ and $b = -1.5$. Plotted along the vertical axis is the amplitude $|\phi|$ (actually, $2|\phi|$) of the mode with wavenumber $k = 1$. The numerical results are indicated by the circles (see text).

different orders of ϕ occurring in each equation, and we can then successively calculate all $u_i^{(j)}$ and C_i. Combining the ϕ^2 parts of Eqs. (21a) and (23) gives

$$u_0^{(2)} = 2b/(2\sigma_1 - \sigma_0), \tag{25}$$

and doing the same for (21b) and (24a) we find

$$u_2^{(2)} = b/(2\sigma_1 - \sigma_2). \tag{26}$$

From Eq. (20) we then deduce that

$$C_3 = 2b(u_0^{(2)} + u_2^{(2)}) + 3c = 2b^2\left(\frac{2}{2\sigma_1 - \sigma_0} + \frac{1}{2\sigma_1 - \sigma_2}\right) + 3c. \tag{27}$$

Note that this means that C_3 depends on ϵ. To lowest order, the transition is subcritical if $C_3 > 0$ at $\sigma_1 = 0$. This implies that

$$\epsilon = (k^2 - 1)^2 \tag{28}$$

and

$$\frac{2}{3}\frac{b^2}{c} > -\left(\frac{2}{\sigma_0} + \frac{1}{\sigma_2}\right)^{-1}. \tag{29}$$

Inserting the expressions for σ_0 and σ_2, we find

$$C_3 = 2b^2\left(\frac{2}{\epsilon + 1} + \frac{1}{\epsilon + 9}\right) + 3c \tag{30}$$

and the condition for subcritical behavior of the least stable mode becomes Eq. (29) at $\epsilon = 0$,

$$b^2/c > -27/38. \tag{31}$$

For $c = -1$, this means that we need $|b| > 0.8429\ldots$ for subcritical behaviour.

Method II. For Method II, we put the left hand side of Eqs. (21a)–(21c) to zero. We then find

$$u_0^{(2)} = \frac{2b}{\sigma_0} = \frac{2b}{1 - \epsilon} \tag{32}$$

and

$$u_2^{(2)} = \frac{b}{\sigma_2} = \frac{b}{9 - \epsilon}, \tag{33}$$

giving

$$C_3 = 2b\left(\frac{2b}{1 - \epsilon} + \frac{b}{9 - \epsilon}\right) + 3c = 2b^2\left(\frac{2}{1 - \epsilon} + \frac{1}{9 - \epsilon}\right) + 3c. \tag{34}$$

The transition to subcritical behavior takes place at the same b^2/c as for Method I.

3.3. Results for both methods up to ninth order

The results for this order and higher order (up to ϕ^9) are represented graphically in Fig. 5, where we plot the amplitude of the $k = 1$ mode as a function of the control parameter ϵ. The lines represent the stationary (either stable or unstable) solutions for the amplitude expansion (9); the circles denote the numerical results. The latter were obtained using a second-order Crank–Nicholson semi-implicit finite-difference scheme [51,52]. We used a domain $x \in [-25\pi, 25\pi]$, which was discretized into 2000 points, giving a spatial stepsize $\Delta x \approx 0.079$. Periodic boundary conditions were used. The initial condition was sinusoidal, with wavenumber $k = 1$, and it was integrated with a timestep $\Delta t = 0.1$. For the stable branch, we started with an initial condition with relatively large amplitude, which was integrated until the solution was (almost) stationary. On this state we performed a discrete Fourier transformation to extract the amplitude of the $k = 1$ mode. The points of the unstable branch were determined by finding the minimal amplitude for which the initial condition grew instead of decaying; they represent a kind of threshold amplitude. This threshold was determined manually to an accuracy of 0.01 in $2|\phi|$.

We see that both expansion methods have difficulty approximating the "true" bifurcation diagram. To order ϕ^5 they both give qualitatively correct results, but to higher orders, the quantitative performance does not improve, and the qualitative behavior actually becomes worse. This holds in particular for Method I, but also Method II starts to show spurious solutions, zeros and divergences. Most of these problems can be explained, but we shall postpone that until after we treat the next example, where similar problems will be encountered.

We do note already at this stage, however, that in Method II the upper branch of nonlinear stable stationary solutions always ends rather abruptly in a divergent way. A similar divergence was also observed in the analysis of nonlinear travelling wave solutions in parallel viscoelastic flows [14,15]. The present analysis lends support to the idea that such a divergence is nonphysical, and simply due to the breakdown of the present mode expansion. Numerical analysis suggests that the values of ϵ at which these divergences occur, converge for high orders. The divergences appear to be related to unexpected zeros in the the highest-order coefficient in our expansion. However, we have not further investigated the cause of these divergences, and their possible significance.

4. Subcritical transition to weak chaos

In this Section, we consider a much richer system, where we encounter a subcritical transition to weak spatiotemporal chaos of Kuramoto–Sivashinsky type. Our motivation for doing so is

the following. As we explained in the introduction, quite often in complex spatiotemporally extended systems the (weakly) chaotic or turbulent dynamics is organized around exact spatially periodic solutions; in parallel shear flows in Newtonian fluids, where this also happens [13,12], the laminar base flow shows no linear instability so the phase diagram is reminiscent of that of Fig. 1(c), what we termed the bifurcation from infinity scenario. Our recent attempt [14,15] to establish a similar scenario for visco-elastic fluids using an amplitude expansion for the periodic travelling wave solutions led us to investigate this approach in a simpler situation with subcritical spatiotemporal chaos.

The outline of this Section is as follows. We will first present the "classical" Kuramoto–Sivashinsky equation, and we then construct an extension of which one can easily convince oneself that it will show a subcritical transition from the trivial solution to spatiotemporal chaos. We investigate the phenomenology of this equation using numerical simulation, and we find that it indeed shows a subcritical transition. We then apply the amplitude expansion to the equation, and we find that while Method II faithfully reproduces the subcritical behavior, Method I seems to perform rather less well, even if the least stable mode is close to criticality. A more detailed analysis of both expansions reveals that the failure of Method I is related to the resonances that occur in Poincaré–Dulac normal forms for ordinary differential equations [43,44,4]. This may have implications for the analysis performed in [14,15].

4.1. Construction of the equation

The Kuramoto–Sivashinsky (KS) equation is a partial differential equation that has been studied extensively as a model for one-dimensional spatiotemporal chaos, both as a (crude) model for physical and chemical processes [19–21,53] and as an interesting model equation in its own right [1,53]. It is a fourth-order equation, given in its "differential" form as

$$\frac{\partial u}{\partial t} = -\gamma \frac{\partial^4 u}{\partial x^4} - \alpha \frac{\partial^2 u}{\partial x^2} + u \frac{\partial u}{\partial x}. \tag{35}$$

The coefficients $\alpha > 0$ and $\gamma > 0$ can be thought of as determining a long-wavelength instability (α) and short-wavelength dissipation (γ) [54].

A linear damping term can be added to this equation, and it can be rescaled to bring the linear part into "Swift–Hohenberg form". The resulting *damped* or *stabilized* Kuramoto–Sivashinsky equation then reads [1,55,56]

$$\frac{\partial u}{\partial t} = -\frac{\partial^4 u}{\partial x^4} - 2\frac{\partial^2 u}{\partial x^2} - u + \epsilon u + u \frac{\partial u}{\partial x}. \tag{36}$$

This equation shows a supercritical (forward) bifurcation to a regular periodic pattern at $\epsilon = 0$. This state becomes unstable with respect to secondary instabilities at $\epsilon_c \approx 0.7$ (depending on the wave number) [57,55], giving rise to chaotic behavior. For $\epsilon = 1$, we have the KS equation proper. Our aim is to find a modification that shows a subcritical transition from the trivial solution to a chaotic state. Adding a lower-order nonlinearity, as we did for the Swift–Hohenberg equation in the previous section, does not work. Instead, we supplement the system with an auxiliary equation, to obtain the following system of two coupled partial differential equations:

$$\frac{\partial u}{\partial t} = -\frac{\partial^4 u}{\partial x^4} - 2\frac{\partial^2 u}{\partial x^2} - u + \epsilon u + (1-\epsilon) f(v) u + u \frac{\partial u}{\partial x}, \tag{37a}$$

$$\frac{\partial v}{\partial t} = D \frac{\partial^2 v}{\partial x^2} - v + R u^2, \tag{37b}$$

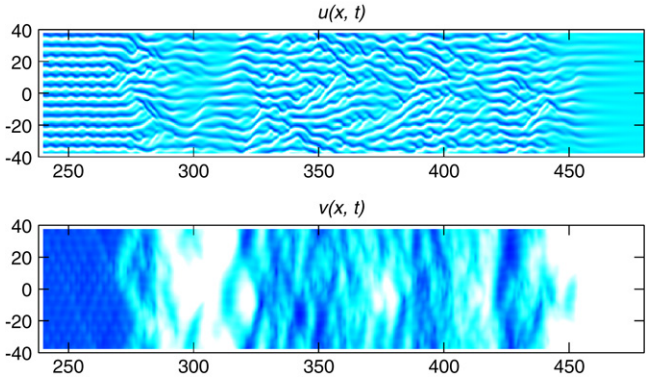

Fig. 6. Typical behavior of the extended damped KS equation as demonstrated by space–time plots for u and v. The initial periodic state undergoes a secondary instability to spatiotemporal chaos, then decays to the trivial state.

where $f(v)$ is a function of v that we will describe below, $D > 0$ and $R > 0$ are constants. The rationale behind this construction is that we would like to have an equation that approximates the KS equation for relatively large amplitudes, and yet is linearly stable (that is, for small amplitudes).

The equation for v contains a diffusion term with a diffusion constant D, which we assume to be large. In the limit $D \to \infty$, we would have $v(x,t)$ constant in x. There is a linear decay term and a driving term Ru^2. Hence, for large D, the auxiliary field v is effectively determined by $\langle u^2 \rangle(t)$, where $\langle \cdot \rangle$ denotes a spatial average. Since v is more or less constant in x, it effectively modifies the linear term in Eq. (37a), through the function $f(v)$.

It should now be possible to choose R and $f(v)$ such as to obtain subcritical behavior. Without loss of generality, we can choose $R = 1$. To obtain a linearly stable trivial solution for $\epsilon < 0$, we require that $f(v) = 0$ for $v = 0$. Then, a self-consistent assumption would be that for the $v \approx \langle u^2 \rangle(t)$ corresponding to a chaotic solution of the original KS equation on a large interval, $f(\langle u^2 \rangle) \approx 1$, so that Eq. (37a) assumes the traditional KS form. To ensure that the system does not "run away", we also require that that for v larger than some maximal $v_{\max}$ we have $f(v) < 0$.

An explicit form for $f(v)$ that can meet these requirements is

$$f(v) = a\, v + b\, v^2 \quad \text{with } a > 0 \text{ and } b < 0. \tag{38}$$

In practice, choosing a and b requires some experimentation, because not only should there be a persistent chaotic solution, but the regular periodic state that appears first needs to have a secondary instability that takes it to the chaotic solution. We will fix a and b, and use ϵ and R as control parameters.

4.2. Phenomenology of the coupled Kuramoto–Sivashinsky-type equation

A first impression of the dynamics of the equation is obtained by numerical simulation using the `NDSolve` function of the computer algebra system *Mathematica*. For definiteness, we chose $D = 40.0$, $a = 0.125$, $b = -0.004$, $\epsilon = -0.1$ (subcritical), $R = 1.0$. We used a domain $x \in [-12\pi, 12\pi]$ with periodic boundary conditions, and initial conditions $u(x,0) = 2.0\cos x + 0.03\cos((11/12)x)$, $v(x,0) = 0.0$. The second term in the initial condition for u serves to 'precipitate' the secondary instability to spatiotemporal chaos. Plots for $u(x,t)$ and $v(x,t)$ are given in Fig. 6, and confirm the 'usual' scenario: first, for sufficiently large initial conditions with a certain wavenumber, a regular patterned state with a constant amplitude (not shown in the plot), then this state starts to show a secondary instability (the wiggles on top of the regular pattern around $t = 250$). At some point, a phase-slip occurs, and a spatiotemporally chaotic state appears. Especially on short

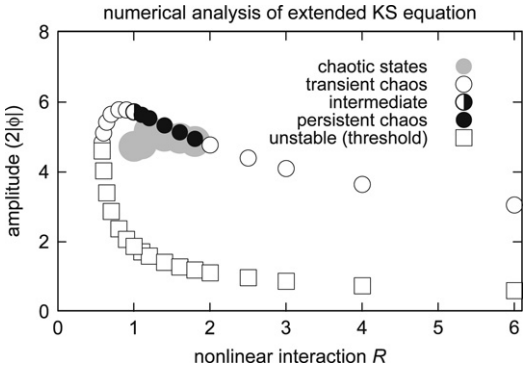

Fig. 7. Diagram summarizing the behavior of the extended KS equation. Squares are 'threshold amplitudes', corresponding to an approximate solution that is unstable. Circles are (at least initially) stable solutions that may show a secondary instability. The gray dots indicate the amplitude of chaotic states (see text).

domains, such as here, this state is prone to sudden extinction. Around $t = 300$ we see such an event nearly happening. Around $t = 450$, the pattern completely disappears. If the initial condition has a lower amplitude (in this case, smaller than about 2) the initial pattern does not grow but decays; the value 2 is then close to the threshold amplitude.

For a more thorough and reproducible investigation, we again used a second-order Crank–Nicholson semi-implicit finite-difference scheme [51,52]. We investigated the behaviour for a range of R between 0.0 and 6.0, at $\epsilon = -0.1$ (other parameters as above). The finite-difference grid consisted of 2000 points on a domain of length 96π (that is, $\Delta x \approx 0.151$), the timestep was fixed at $\Delta t = 0.1$. The results are summarized in Fig. 7. Open squares denote unstable approximate solutions (threshold), the circles correspond to $2|\phi|$, with ϕ the amplitude of the $k = 1$ mode as determined by taking a discrete Fourier transform of the regular pattern to which the equation initially converges, and their filling indicates whether the resulting chaotic state is persistent or transient. All cases are prone to secondary instabilities, but only for $R \leq 1.1$ is the pattern with $k = 1$ unstable. In the other cases, only lower wavenumber patterns are unstable.

For $1.0 \leq R \leq 2.0$, persistent spatiotemporal chaos can occur, and the gray "blobs" in the graph are a rough indication of the average amplitude of these chaotic states. These averages were obtained by sampling chaotic waveforms at certain time intervals and averaging over their root mean square (RMS) amplitudes.[4] They are drawn rather large to indicate that on short and intermediate domains this value can fluctuate appreciably.

For lower R, transient chaos may appear but it will eventually decay to the trivial solution. For larger R, it will decay to a regular patterned state, if chaos appears at all.

There is one additional phenomenon that warrants attention. For smaller diffusion constant ($D \approx 10$), transient chaos may for lower R decay either to the trivial solution or to a state consisting of uniformly travelling pulses. There are single pulses as well as multi-pulse solutions called *bound states* in the terminology of Malomed et al. [58], who observed pulses in a different extension of the KS equation. As shown in Fig. 8, the pulses that we find are approximate homoclinic orbits, and their structure resembles the homoclinic orbit solutions (*homoclons*) [59] of the complex Ginzburg–Landau equation and the so-called *Shil'nikov loop* [44] (actually, an 'inverse' Shil'nikov loop [60,61]: at a certain point in space, as the pulse passes, the field first oscillates, then comes back to zero again). Such loops appear to be connected to the emergence of spatiotemporal chaos [62] and strange attractors [44,60,61].

Since secondary instabilities, chaos and pulses are phenomena that cannot be captured by our amplitude expansion formalism, we shall not say more about these. The numerical analysis clearly indicates that our extension of the KS equation shows the behavior sought for (i.e., a subcritical transition to weakly spatiotemporally chaotic states), and we proceed to investigate to what extent we can capture the gross features of these chaotic branches with a simple mode expansion.

4.3. Amplitude expansion

The extended KS equation that we consider can be reduced to an amplitude equation because it has a clear separation of time scales for $|\epsilon| \ll 1$. The linearly least stable eigenmode of the linear part of the equation is $u(x) = e^{ix}$, $v(x) = 0$, which decays as $e^{\epsilon t}$. Of course, modes with slightly different wavenumber will have only slightly smaller eigenvalues, but in the spirit of this expansion, we choose a mode, and perturbatively probe periodic solutions with the same wavelength. The higher order harmonics that are generated from the basic mode through the nonlinear interactions are well separated from the near-critical mode, and therefore, a description in terms of the amplitude ϕ of the near-critical mode may work.

For the amplitude expansion, the present equation is considerably more complicated than the generalized Swift–Hohenberg equation from Section 3: there are two equations, and there are more nonlinearities. We will carry out the expansion explicitly to order C_3, and rely on a computer algebra system to go to higher orders.

First, we have to deal with the fact that here we have two fields instead of one. A transparent way to deal with this is to consider the U_n and the $u_i^{(j)}$ as vectors instead of scalars. We can then write the relevant equations as

$$\begin{aligned}\mathbf{w}(x,t) &= (u(x,t), v(x,t)) \\ &= \phi(t)\mathbf{Y}_1 e^{ikx} + \phi^*(t)\mathbf{Y}_{-1}e^{-ikx} \\ &\quad + \mathbf{W}_0(t) + \sum_{n=2}^{\infty}\left[\mathbf{W}_n(t)e^{inkx} + \mathbf{W}_{-n}(t)e^{-inkx}\right], \end{aligned} \tag{39}$$

where $\mathbf{W}_n = (U_n, V_n)$ and $\mathbf{Y}_1 e^{inkx}$ is a (near-) critical mode with $\mathbf{Y}_1 = (1, 0)$. Note that we chose $(1, 0)$ since that is the least stable eigenvector for the linear part of the system. Furthermore,

$$\mathbf{W}_0(t) = \mathbf{W}_0(\phi) := \mathbf{w}_0^{(2)}|\phi|^2 + \mathbf{w}_0^{(4)}|\phi|^4 + \cdots \tag{40}$$

analogous to the equations from Section 2, but in vector form. We can also write this in a more *ad hoc* component notation using $u_i^{(j)}$ and $v_i^{(j)}$, especially since there are no eigenfunctions of $\mathcal{L}$ that involve both the u and the v component. At any rate, there will not be any "V_1" terms.

Including all equations and terms necessary for computing C_3, we find

$$\frac{d\phi}{dt} = \epsilon + iU_0\phi + iU_2\phi^* + (1-\epsilon)aV_0\phi + (1-\epsilon)aV_2\phi^* + \cdots, \tag{41a}$$

$$\frac{dU_0}{dt} = (\epsilon - 1)U_0 + \cdots \tag{41b}$$

$$\frac{dU_2}{dt} = (\epsilon - 9)U_2 + i\phi^2 + \cdots, \tag{41c}$$

$$\frac{dV_0}{dt} = R|\phi|^2 - V_0 + \cdots, \tag{41d}$$

$$\frac{dV_2}{dt} = R\phi^2 - V_2 - 4DV_2 + \cdots. \tag{41e}$$

[4] Actually, the symbols denote $\sqrt{2}$ times the RMS amplitude, to make this compatible with the $2|\phi|$, which for the $k = 1$ mode is also $\sqrt{2}$ times the RMS amplitude.

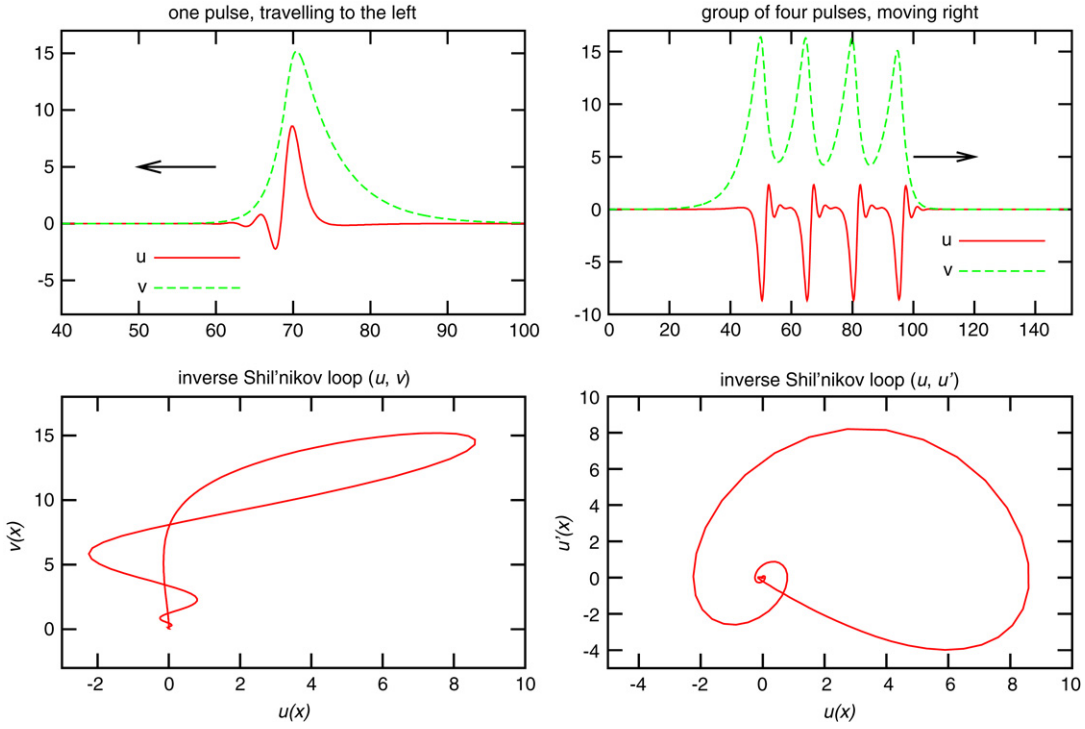

Fig. 8. For smaller diffusion constants, pulses may arise out of transient chaos. The pulses we find are uniformly translating, they appear to be stable, and they may occur alone or in groups. The lower two plots show the spatial structure of the single pulse at a fixed time, as a parametric plot in x, for two different projections. The structure is an approximate homoclinic orbit, reminiscent of a Shil'nikov loop, but reversed. Parameter values used were $D = 10.0$, $R = 0.97$, $\epsilon = -0.1$, $a = 0.125$ and $b = -0.004$.

For an expression for C_3 we write out the equation for ϕ in terms of $u_i^{(j)}$ and $v_i^{(j)}$:

$$\frac{\mathrm{d}\phi}{\mathrm{d}t} = \epsilon\phi + \mathrm{i}u_0^{(2)}|\phi|^2\phi + \mathrm{i}u_2^{(2)}|\phi|^2\phi + (1-\epsilon)av_0^{(2)}|\phi|^2\phi + (1-\epsilon)av_0^{(2)}|\phi|^2\phi + \cdots \tag{42}$$

and we find

$$C_3 = \mathrm{i}(u_0^{(2)} + u_2^{(2)}) + (1-\epsilon)a(v_0^{(2)} + v_2^{(2)}). \tag{43}$$

We can then calculate this using both Method I and Method II.

Expanding the right hand side of Eqs. (41a)–(41e) as well as the time derivatives, we find to order ϕ^2

$$2u_0^{(2)}\epsilon|\phi|^2 = (\epsilon - 1)u_0^{(2)}|\phi|^2, \tag{44a}$$

$$2u_2^{(2)}\epsilon\phi^2 = (\epsilon - 9)u_2^{(2)}\phi^2 + \mathrm{i}\phi^2, \tag{44b}$$

$$2v_0^{(2)}\epsilon|\phi|^2 = R|\phi|^2 - v_0^{(2)}|\phi|^2, \tag{44c}$$

$$2v_2^{(2)}\epsilon\phi^2 = R\phi^2 - v_2^{(2)}\phi^2 - 4Dv_2^{(2)}\phi^2. \tag{44d}$$

For *Method I* we solve these equations, to obtain

$$u_0^{(2)} = 0, \qquad u_2^{(2)} = \frac{\mathrm{i}}{9+\epsilon}, \qquad v_0^{(2)} = \frac{R}{1+2\epsilon}, \qquad v_2^{(2)} = \frac{R}{1+2\epsilon+D}, \tag{45}$$

and

$$C_3 = -\frac{1}{9+\epsilon} + (1-\epsilon)aR\left(\frac{1}{1+2\epsilon} + \frac{1}{1+2\epsilon+D}\right). \tag{46}$$

For *Method II* we put the left hand side of the equations to zero, and we find

$$u_0^{(2)} = 0, \qquad u_2^{(2)} = \frac{\mathrm{i}}{9-\epsilon}, \qquad v_0^{(2)} = R, \qquad v_2^{(2)} = \frac{R}{1+D}, \tag{47}$$

and

$$C_3 = -\frac{1}{9-\epsilon} + (1-\epsilon)aR\left(1 + \frac{1}{1+D}\right). \tag{48}$$

For higher orders, as mentioned, we have to resort to computer algebra programs. We will not give explicit analytic expressions for the coefficients: these can easily be obtained, but they add little to our understanding of what goes on.

For the values chosen in our numerical analysis ($D = 40, R = 1$, $a = 0.125, \epsilon = -0.1$) we have compared the amplitude expansion to the numerics, up to and including ninth order in the amplitude and this is shown in Fig. 9. It is clear that the threshold amplitude (that is, up to third order) is predicted quite well by both methods. At fifth order, however, we clearly see that *Method I* breaks down completely—going to higher order does not improve this in any way, as we already observed for the extended Swift–Hohenberg equation. Method II, on the other hand, performs very well: both branches are accurately determined for all values of R shown.

5. Discussion

In the previous sections we analyzed the application of the amplitude expansion to two different systems in two different forms. At first sight these results may look rather inconsistent or inconclusive. Indeed, there is a sharp contrast between the success of Method II on the extended Kuramoto–Sivashinsky equation and the complete failure of Method I on that equation.

There are two possible general explanations for this: (i) the concepts of slaving, separation of timescales and slow manifolds do not apply to these systems or (ii) the concepts are valid, but the problem is in the actual approximation of the slow manifold. In the cases we considered, the problem is definitely in the actual approximation. That the concept of slow manifolds is valid, can be seen from Fig. 10. We followed the behavior of the extended Swift–Hohenberg equation for a variety of initial

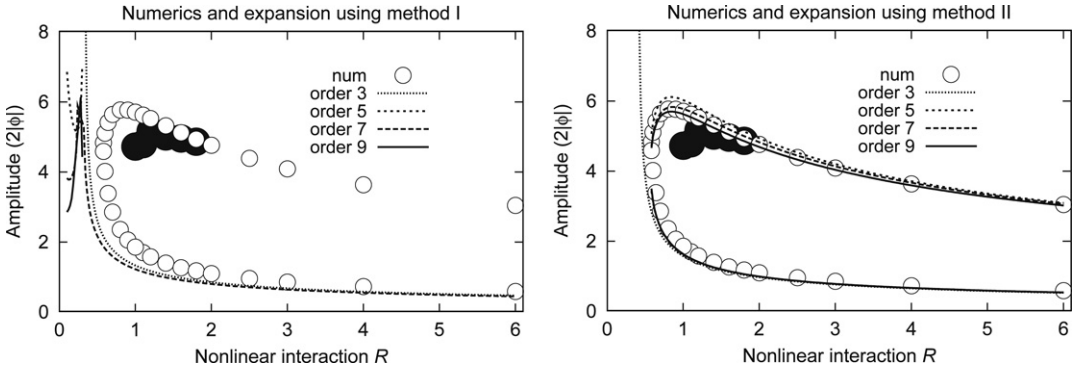

Fig. 9. Comparison of our amplitude expansions Method I and Method II with numerical results. The left plot shows our results up to ninth order for Method I, the right one for Method II. The numerical data is the amplitude of the $k = 1$ mode, as obtained by a discrete Fourier transform of the actual waveform, while the expansion data shows $\phi + \phi^*$, which is $2|\phi|$ for this case. The gray blobs again indicate the amplitude of chaotic solutions ($\sqrt{2}$ times the RMS amplitude).

conditions consisting of the $k = 1$ mode plus some admixture of harmonics ($k = 0, 2, 3$), and we separated the spectral content as a function of time into the basic mode ($k = 1$) and the harmonics. To be more specific: starting from the initial conditions, the actual waveform can be written as

$$u(x, t) = \sum_{n=-\infty}^{+\infty} U_n(t) \exp[inkx], \tag{49}$$

where U_1 corresponds to the amplitude ϕ. We can now define a *root mean square* amplitude of the dominant mode as

$$A_1(t) = \sqrt{|U_1|^2 + |U_{-1}|^2} = \sqrt{2|U_1|^2}. \tag{50}$$

The total amplitude is defined as the $\mathcal{L}_2$ norm of $u(x, t)$ on the domain $x \in [-\pi, \pi]$ at time t, so we have

$$A_{\text{total}}(t) = \|u(x, t)\| = \sqrt{U_0^2(t) + 2|U_1(t)|^2 + 2|U_2(t)|^2 + 2|U_3(t)|^2 + \cdots} \tag{51}$$

and we define the effective amplitude of the modes other than $k = 1$ as

$$A_{\text{other}}^2(t) = A_{\text{total}}^2(t) - A_1^2(t). \tag{52}$$

In Fig. 10 we plot on the horizontal axis the amplitude of the dominant $k = 1$ mode, $A_1(t)$, and on the vertical axis the total effective amplitude of the other modes, $A_{\text{other}}(t)$, as well as the approximate fixed points. The coefficients $U_i(t)$ were obtained by numerical integration of the extended Swift–Hohenberg equation and applying at certain times a discrete Fourier transformation to the discretized waveform. It is clear that there is a slow manifold to which all solutions converge, at least between the origin and the stable nontrivial solution.

What then is the problem with the approximation of this manifold? What the two methods have in common, is that they both attempt a power series approximation. While this seems a natural approach, there is no guarantee that the radius of convergence of such series is sufficiently large to capture the relevant amplitudes, or indeed that they converge at all. In fact, even though we are focusing on a mode expansion – not on a full-fledged amplitude equation which allows for spatial modulation – we should keep in mind that amplitude descriptions are typically *asymptotic methods*, that is, the radius of convergence is formally zero and beyond some point, the results get *worse* as more terms are included in the expansion [63].

That power series expansions in amplitude approaches are problematic, was realized earlier by Herbert [31], who attempted a high-order amplitude expansion for the nonlinear stability of plane Poiseuille flow, and by Fraser [26] in the context of slow manifolds

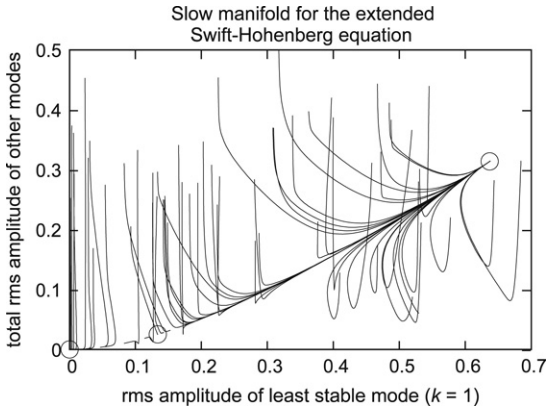

Fig. 10. Existence of the slow manifold for the extended Swift–Hohenberg equation (14) with $\epsilon = -0.05$, $b = 1.5$, $c = -1.0$, on a domain $x \in [-\pi, \pi]$, with t running from 0 to 20. Along the horizontal axis we plot the amplitude of the $k = 1$ part of the solution as a function of time, while along the vertical axis the effective amplitude of all other harmonics is plotted, see text. Solutions clearly converge to a slow manifold for a variety of initial conditions. The open circles indicate (approximate) stationary solutions.

for chemical kinetics, without, however, giving a satisfactory explanation for the occurrence of these problems.

More insight into this can be gained if we realize that, at least formally, the amplitude equation (9) may also have complex solutions, even though they are not physical (the amplitude equation can be separated in a part for the modulus and the argument of the complex amplitude, and these solutions would correspond to a complex modulus). Looking then at Fig. 11, we see that problems, such as the spurious zero in the left panel ($\epsilon = -1/3$) and the spurious divergence in the right panel ($\epsilon \approx 0.52$), are literally connected to these complex solutions.

5.1. Method I: Connection to normal forms and resonances

For Method I, an interpretation can be given in terms of Poincaré–Dulac normal forms. Although the method is not strictly the same as a normal form reduction, the underlying idea is the same: to find a nonlinear coordinate transformation that simplifies the system such that nonlinearities essentially only occur in one variable [43], in our case the amplitude ϕ. However, such transformations suffer from *resonances*: if eigenvalues of the linear part of the equation satisfy certain relations, the method breaks down, and this appears to be precisely what happens here. The first example of this can be seen in our expansion to order ϕ^3: the explicit expansion of the time derivative of mode U_0 causes the denominator of the corresponding coefficient $u_0^{(2)}$ to be zero

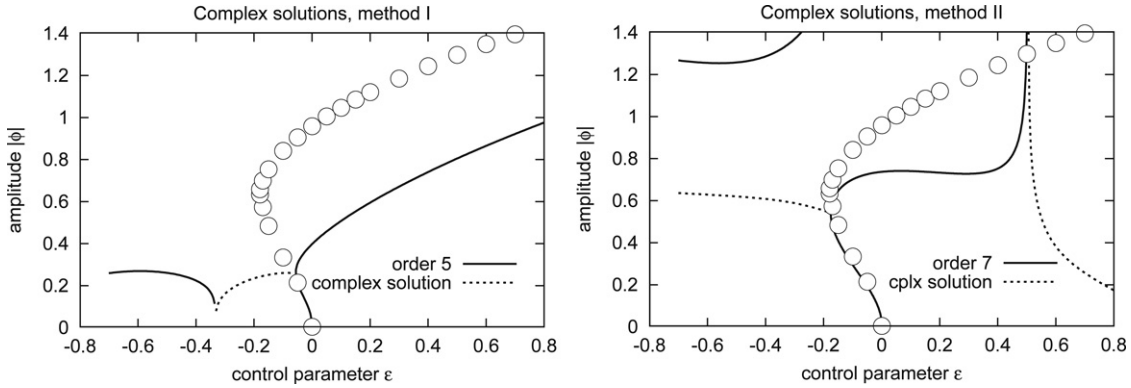

Fig. 11. Results for the amplitude expansion of the extended Swift–Hohenberg equation with $b = 1.5$ and $c = -1.0$, for Method I and Method II. Now, also the complex (unphysical) solutions are included. Note that the order is different for both methods (orders 5 and 7, respectively). The complex solutions for method I are clearly connected to the resonances discussed in the text. For method II, the complex solutions are related to (unphysical) divergences in the amplitude that are caused by spurious zeros of the C_i as functions of ϵ. The connection to the subcritical "nose" of the bifurcation diagram is of course correct, and unavoidable.

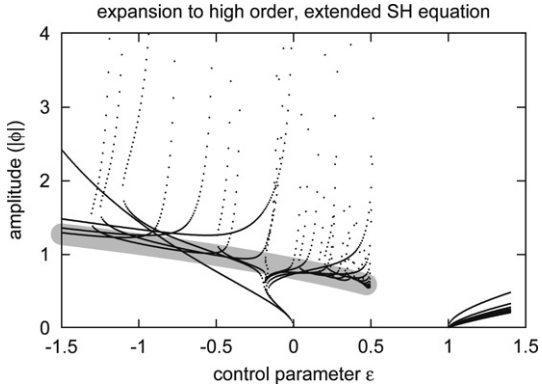

Fig. 12. Results for Method II applied to the extended Swift–Hohenberg equation, up to order ϕ^{21}, without distinguishing the different orders. We clearly see problems at $\epsilon = 1.0$ and $\epsilon \approx 0.5$. However, the behavior of the expansion suggests that for $\epsilon < 0.5$, the series does converge and has a finite radius of convergence, roughly indicated by the gray area, which is a guide to the eye.

at $\epsilon = -1$. This becomes more severe for higher orders: for example, for $O(\phi^5)$, a term with denominator $3\epsilon + 1$ appears, when on the left hand side of Eq. (23) a term $4u_0^{(4)}\sigma_1|\phi|^4$ occurs. Zero denominators lead to infinite values for coefficients $u_i^{(j)}$, and hence to unwanted infinities in the C_i, leading in turn to spurious zeros for the amplitude ϕ. The resonance condition corresponding to the $u_0^{(4)}$ case would be $\sigma_1 = 4\sigma_1 + \sigma_0$, and the resonance is then of order 5 [43]. Indeed, looking back at Fig. 5, we can clearly see the resonances "marching in" from the left, at $\epsilon = -1, -1/3, -1/5, -1/7, \ldots$ as we go to higher order.

In fact, even if the resonances occur at ϵ substantially away from the region of interest, these resonances may destroy the approximation. Already in Fig. 11, we see that the "nose" of the diagram is "pulled down" by the complex connection to the resonance. This is even more dramatic in the case of the application of Method I to the extended Kuramoto–Sivashinsky equation: although for order $O(\phi^5)$ there is only a resonance at $\epsilon = -1/4$, already for $\epsilon = -0.1$ the approach completely breaks down, in the same way as for the extended Swift–Hohenberg equation.

5.2. Method II: Convergence and spurious zeros

For Method II, these resonances do not occur since the time derivative is not expanded, and no higher multiples of ϵ occur. However, for the extended Swift–Hohenberg equation we clearly see two problems: there appears to be a finite range in ϕ that can be reliably approximated, and there appear spurious solutions and spurious behavior, for example the unphysical solution in the upper left corner of Fig. 5 or the sudden increase of the amplitude for $\epsilon \approx 0.5$.

The first of these problems has to do with the convergence of the method. It is not clear whether the expansion converges at all. However, Fig. 12 indicates that the series may actually converge. We plot the stationary solutions for expansions up to and including order ϕ^{21}, without distinguishing the different orders. The results are consistent with a finite radius of convergence that depends on ϵ, and would be around $|\phi| \approx 0.8$ for $\epsilon = 0$. This, however, is still smaller than the amplitude of the nontrivial stable stationary solution, and this stable branch cannot be captured numerically accurately by pursuing the expansion to high order. Despite the indications that the series may converge, it is difficult to actually show this. The coefficients C_i seem to jump around unpredictably, at least in the subcritical region of interest, and simple convergence tests do not apply. More sophisticated methods such as Padé approximants [63] may be able to shed more light on this, and for reference we have listed numerical values of the coefficients in Appendix, for Method II as well as for Method I.

In any case, the expansion clearly does not get us very far since (i) the U_0 mode has a relatively slow linear decay, and (ii) it has a rather large forcing through the u^2 term. Both aspects are important, and simple linear considerations cannot predict this behavior.

Then there is the problem of spurious divergences in the amplitude, as in the right panel of Fig. 11. Clearly here too the spurious behavior is associated with an unphysical complex solution. This behavior is caused by unexpected zeros of the coefficients C_i: these coefficients depend on ϵ and for certain values of ϵ, one or more of the C_i becomes zero. If the highest C_i at the order we are considering becomes zero, that leads to an unphysical infinity of the amplitude. It is not a priori clear where these zeros occur, or what precisely causes them. One way of dealing with this problem would be to explicitly remove the ϵ dependence of the C_i by taking $\epsilon \to 0$ after calculating the coefficients and keeping ϵ only in the linear part of the amplitude equation. However, that does not solve the convergence problem, and it still may limit the range in ϵ that can be covered.

5.3. Methods without power series

Especially in problems of chemical kinetics (such as combustion and reactive flows) methods have been devised to circumvent the problems with power series expansions of the slow manifolds. These sophisticated methods are quantitatively accurate, and

Table A.1
Coefficients for subcritical Swift–Hohenberg equation, Method I, for different ϵ.

	$\epsilon = -1.4$	$\epsilon = -0.4$	$\epsilon = 0.0$	$\epsilon = 0.4$
C_3	−24.9079	12.5233	6.5	3.90729
C_5	86.5722	1693.07	−166.961	−50.3805
C_7	237.125	105095	6936.5	546.23
C_9	−51001.3	9.82861×10^6	−465375	−7930.86
C_{11}	1.96347×10^6	9.62723×10^8	4.09738×10^7	133298
C_{13}	-5.59912×10^7	1.02842×10^{11}	-4.34026×10^9	-2.44041×10^6
C_{15}	1.34439×10^9	1.14367×10^{13}	5.28829×10^{11}	4.72549×10^7
C_{17}	-2.76036×10^{10}	1.31755×10^{15}	-7.21751×10^{13}	-9.51949×10^8
C_{19}	4.63707×10^{11}	1.55593×10^{17}	1.0847×10^{16}	1.9749×10^{10}
C_{21}	-5.3405×10^{12}	1.87464×10^{19}	-1.77413×10^{18}	-4.19115×10^{11}

Table A.2
Coefficients for subcritical Swift–Hohenberg equation, Method II, for different ϵ.

	$\epsilon = -1.4$	$\epsilon = -0.4$	$\epsilon = 0.0$	$\epsilon = 0.4$
C_3	1.18269	3.90729	6.5	12.5233
C_5	−14.5037	−32.6767	−49.2383	−52.3656
C_7	33.3087	62.0359	7.16139	−406.853
C_9	−32.7639	206.779	893.679	−3447.39
C_{11}	−98.0557	−1294.58	1277.23	−18512.5
C_{13}	509.173	−1922.02	−32780.8	122961.
C_{15}	−730.749	32236.7	−126699.	5.40599×10^6
C_{17}	−2184.14	−6537.84	1.38485×10^6	9.11323×10^7
C_{19}	13516.4	−841285.	9.92885×10^6	9.49964×10^8
C_{21}	−21533.6	1.63677×10^6	-5.66105×10^7	3.11774×10^9

are often based on an iterative scheme of some kind [26]. However, our aim is different: eventually we would like to apply amplitude expansion methods to fluid dynamical problems which are defined by two- or three-dimensional partial differential equations. It is not a priori clear that these iterative schemes can be successfully generalized to partial differential equation without the computational cost becoming excessive. Furthermore, we do not necessarily aim at a quantitatively accurate answer; we would in principle just like to know whether a finite-amplitude instability is to be expected for a given system. These approximation schemes do not seem an obvious choice for that purpose.

6. Conclusions

In this paper, we have explored two explicit implementations of an amplitude expansion method for partial differential equations with a clear separation of timescales, with the aim of getting some insight into the interpretation of results of such expansions in complex spatiotemporal problems where one suspects a subcritical bifurcation or a bifurcation from infinity [15]. We have investigated and tentatively discussed the limits of the applicability of the methods by applying them to two different systems with a subcritical nonlinear instability. While the methods cannot in general be used for obtaining quantitatively accurate nontrivial stationary solutions, and even the qualitative performance may completely break down at high orders in the amplitude, the methods (in particular the one we call Method II) can be of good use if one needs limited, qualitative information, and provided it is applied with caution. Most importantly, for low orders in the amplitude (third or fifth order) Method II gives robust results when it comes to predicting the possible existence of nonlinear (finite-amplitude) instabilities. This works because the concept of the so-called slow manifold is meaningful for these systems and, at low order in the amplitude, the method does not yet run into the problems associated with high-order amplitude expansions.

By comparing Methods I and II with the exact solutions for simple model equations, where such solutions could be found without much effort, we wanted to assess whether those methods could be used for predicting exact non-linear states in hydrodynamic problems, especially in parallel shear flows of both Newtonian and viscoelastic fluids. There, exact states are often travelling waves of the form $\mathbf{v} = \mathbf{v}(x - ct)$, where c is the wave speed of the solution. Our present analysis focuses on stationary bifurcations ($c = 0$) and therefore cannot be applied immediately to traveling waves. It would be of interest to extend our analysis – and in particular method II – to nonlinear travelling waves like those studied in [15]. In the cubic and quintic complex Ginzburg–Landau equation for travelling waves near the supercritical or subcritical instability scenarios of Fig. 1(a) and (b), the "renormalization" of the wave speed c and the group velocity v_{gr} with amplitude is a well-known phenomenon [64] and occurs through the imaginary parts of the coefficients in these equations. This procedure is very much like that in method I and this suggests that the extension of our method I to travelling waves will proceed along similar lines as the analysis in this paper. A preliminary study in the context of the viscoelastic flow problem [15] indicates, however, that a straightforward extension of method II to traveling waves that bifurcate off infinity (the scenario of Fig. 1c) is highly nontrivial and may even be impossible.

Acknowledgments

We are grateful to Martin van Hecke for a discussion which led to propose the coupled Eqs. (37a) and (37b) as a suitable model for investigating a subcritical bifurcation to weakly chaotic patterns, and to Arjen Doelman and Vivi Rottschäfer for illuminating remarks. Moreover, ANM is grateful to the NWO/FOM programme "Dynamics of Patterns" for funding his postdoc position in Leiden, where most of this work was done. ANM also acknowledges support from the Royal Society of Edinburgh/BP Trust Research Fellowship.

Appendix. Coefficients for the extended Swift–Hohenberg equation

Tables A.1 and A.2 list the numerical values for our expansion of the Swift–Hohenberg equation up to 21st order in the amplitude,

for different values of the control parameter ϵ, for both Method I and Method II. We again used $b = 1.5$, $c = -1.0$, for both methods.

References

[1] M.C. Cross, P.C. Hohenberg, Pattern formation outside of equilibrium, Rev. Modern Phys. 65 (1993) 851–1112.
[2] A.C. Newell, T. Passot, J. Lega, Order parameter equations for patterns, Annu. Rev. Fluid Mech. 25 (1993) 399–453.
[3] M. van Hecke, P.C. Hohenberg, W. van Saarloos, Amplitude equations for pattern forming systems, in: H. van Beijeren, M.H. Ernst (Eds.), Fundamental Problems in Statistical Mechanics vol. VIII, North-Holland, Amsterdam, 1994.
[4] G. Nicolis, Introduction to Nonlinear Science, Cambridge University Press, Cambridge, UK, 1995.
[5] D. Walgraef, Spatio-Temporal Pattern Formation, Springer, New York, 1997.
[6] S. Fauve, Pattern forming instabilities, in: C. Godrèche, P. Manneville (Eds.), Hydrodynamics and Nonlinear Instabilities, Cambridge University Press, Cambridge, UK, 1998.
[7] Y. Nishiura, Far-from-Equilibrium Dynamics, in: Translations of Mathematical Monographs, vol. 209, American Mathematical Society, Providence, R.I., 2002.
[8] R. Hoyle, Pattern Formation, An Introduction to Methods, Cambridge, Cambridge, 2006.
[9] M. Bestehorn, H. Haken, Transient patterns of the convection instability — a model-calculation, Z. Phys. B 57 (1984) 329–333.
[10] A.M. Turing, The chemical basis of morphogenesis, Phil. Trans. R. Soc. Lond. B 237 (1952) 37–72.
[11] S. Rosenblat, S.H. Davis, Bifurcation from infinity, SIAM J. Appl. Math. 37 (1979) 1–19.
[12] R.R. Kerswell, Recent progress in understanding the transition to turbulence in a pipe, Nonlinearity 18 (2005) 17–44.
[13] B. Eckhardt, T.M. Schneider, B. Hof, J. Westerweel, Turbulence transition in pipe flow, Annu. Rev. Fluid Mech. 39 (2007) 447–468.
[14] A.N. Morozov, W. van Saarloos, Subcritical finite-amplitude solutions in plane Couette flow of viscoelastic fluids, Phys. Rev. lett. 95 (2005) 024501.
[15] A.N. Morozov, W. van Saarloos, An introductory essay on subcritical instabilities and the transition to turbulence in visco-elastic parallel shear flows, Phys. Rep. 447 (2007) 112–143.
[16] T. Herbert, Periodic secondary motions in a plane channel, in: Proc. 5th Int. Conf. on Numerical Methods in Fluid Dynamics, Springer, 1976.
[17] S.A. Orszag, A.T. Patera, Subcritical transition to turbulence in planar shear flows, in: Transition and Turbulence, Academic Press, 1981.
[18] B. Meulenbroek, C. Storm, A.N. Morozov, W. van Saarloos, Weakly nonlinear subcritical instability of visco-elastic Poiseuille flow, J. Non-Newtonian Fluid Mech. 116 (2004) 235–268.
[19] G.I. Sivashinsky, Non-linear analysis of hydrodynamic instability in laminar flames. 1. Derivation of basic equations, Acta Astronaut. 4 (1977) 1177–1206.
[20] G.I. Sivashinsky, Instabilities, pattern-formation and turbulence in flames, Annu. Rev. Fluid Mech. 15 (1983) 179–199.
[21] Y. Kuramoto, T. Tsuzuki, Persistent propagation of concentration waves in dissipative media far from thermal equilibrium, Progr. Theor. Phys. 55 (1976) 356–369.
[22] M. Nagata, 3-dimensional finite-amplitude solutions in plane Couette-flow — bifurcation from infinity, J. Fluid Mech. 217 (1990) 519–527.
[23] F. Waleffe, Homotopy of exact coherent structures in plane shear flows, Phys. Fluids 15 (6) (2003) 1517.
[24] H. Wedin, R.R. Kerswell, Exact coherent structures in pipe flow: Travelling wave solutions, J. Fluid Mech. 508 (2004) 333–371.
[25] F. Waleffe, On a self-sustaining process in shear flows, Phys. Fluids 9 (1997) 883.
[26] S.J. Fraser, The steady state and equilibrium approximations: A geometrical picture, J. Chem. Phys. 88 (1988) 4732–4738.
[27] F.G. Heineken, H.M. Tsuchiya, R. Aris, On the mathematical status of the pseudo-steady state hypothesis of biochemical kinetics, Math. Biosci. 1 (1967) 95–113.
[28] L.D. Landau, On the problem of turbulence, Dokl. Akad. Nauk SSSR 44 (1944) 311–314.
[29] J.T. Stuart, On the non-linear mechanics of wave disturbances in stable and unstable parallel flows, J. Fluid Mech. 9 (1960) 353–370.
[30] J. Watson, On the non-linear mechanics of wave disturbances in stable and unstable parallel flows, J. Fluid Mech. 9 (1960) 371–389.
[31] T. Herbert, Nonlinear stability of parallel flows by high-order amplitude expansions, AIAA J. 18 (1980) 243–248.
[32] W. Eckhaus, Studies in Non-Linear Stability Theory, Springer-Verlag, Berlin, 1965.
[33] A.C. Newell, J.A. Whitehead, Finite bandwidth, finite amplitude convection, J. Fluid Mech. 38 (1969) 279–303.
[34] M. Weinstein, Nonlinear instability in plane Poiseuille flow: A quantitative comparison between the methods of amplitude expansions and the method of multiple scales, Proc. R. Soc. Lond. A 375 (1981) 155–167.
[35] K. Fujimura, Methods of centre manifold reduction and multiple scales in the theory of weakly nonlinear stability for fluid motions, Proc. R. Soc. Lond. A 434 (1991) 719–733.
[36] K. Fujimura, Centre manifold reduction and the Stuart–Landau equation for fluid motions, Proc. R. Soc. Lond. A 453 (1997) 181–203.
[37] J. Swift, P.C. Hohenberg, Hydrodynamic fluctuations at convective instability, Phys. Rev. A 15 (1977) 319–328.
[38] H. Haken, Advanced Synergetics, Springer, Berlin, 1983.
[39] M. Hilali, S. Métens, P. Borckmans, G. Dewel, Pattern selection in the generalized Swift-Hohenberg equation, Phys. Rev. E 51 (1995) 2046–2052.
[40] W. van Saarloos, Front propagation into unstable states. II. Linear versus nonlinear marginal stability and rate of convergence, Phys. Rev. A 39 (1989) 6367–6390.
[41] H. Haken, Synergetics—An Introduction, Springer, Berlin, 1977.
[42] C. Foias, G.R. Sell, R. Temam, Inertial manifolds for nonlinear evolutionary equations, J. Differential Equations 73 (1988) 309–353.
[43] V.I. Arnol'd, Geometrical Methods in the Theory of Ordinary Differential Equations, Springer, New York, 1983.
[44] J. Guckenheimer, P. Holmes, Nonlinear Oscillations, Dynamical Systems, and Bifurcations of Vector Fields, Springer, New York, 1983.
[45] W. Wasow, Asymptotic Expansions for Ordinary Differential Equations, Interscience, New York, 1965.
[46] J.J. Levin, N. Levinson, Singular perturbations of non-linear systems of differential equations and an associated boundary layer problem, J. Ration. Mech. Anal. 3 (1954) 247–270.
[47] Y. Pomeau, P. Manneville, Wavelength selection in cellular flows, Phys. Lett. 75A (1980) 296–298.
[48] L.A. Peletier, W.C. Troy, Spatial Patterns: Higher Order Models in Physics and Mechanics, Birkhäuser, Boston, 2001.
[49] G.J.B. Van den Berg, L.A. Peletier, W.C. Troy, Global branches of multi-bump periodic solutions of the Swift–Hohenberg equation, Arch. Ration. Mech. Anal. 158 (2001) 91–153.
[50] L.A. Peletier, V. Rottschäfer, Pattern selection of solutions of the Swift–Hohenberg equation, Physica D 194 (2001) 95–126.
[51] W.H. Press, S.A. Teukolsky, W.T. Vetterling, B.P. Flannery, Numerical Recipes in Fortran 77, 2nd ed., Cambridge University Press, Cambridge, UK, 1992.
[52] B. Fornberg, A Practical Guide to Pseudospectral Methods, Cambridge University Press, Cambridge, UK, 1996.
[53] Y. Kuramoto, Waves, Chemical Oscillations, and Turbulence, Springer, Berlin, 1984.
[54] J.M. Greene, J.-S. Kim, The steady states of the Kuramoto-Sivashinsky equation, Physica D 33 (1988) 99–120.
[55] K.R. Elder, J.D. Gunton, N. Goldenfeld, Transition to spatiotemporal chaos in the damped Kuramoto-Sivashinsky equation, Phys. Rev. E 56 (1997) 1631–1634.
[56] C. Misbah, A. Valance, Secondary instabilities in the stabilized Kuramoto–Sivashinsky equation, Phys. Rev. E 49 (1994) 166–183.
[57] H. Chaté, P. Manneville, Transition to turbulence via spatiotemporal intermittency, Phys. Rev. Lett. 58 (1987) 112–115.
[58] B.A. Malomed, B.-F. Feng, T. Kawahara, Stabilized Kuramoto–Sivashinksy system, Phys. Rev. Lett. 64 (2001) 046304.
[59] M. van Hecke, Building blocks of spatiotemporal chaos, Phys. Rev. Lett. 80 (1998) 1896–1899.
[60] A. Arnéodo, F. Argoul, J. Elezgaray, P. Richetti, Homoclinic chaos in chemical systems, Physica D 62 (1993) 134–169.
[61] N.J. Balmforth, Solitary waves and homoclinic orbits, Annu. Rev. Fluid Mech. 27 (1995) 335–373.
[62] M. van Hecke, M. Howard, Ordered and self-disordered dynamics of holes and defects in the one-dimensional complex Ginzburg–Landau equation, Phys. Rev. Lett. 86 (2001) 218–221.
[63] C.M. Bender, S.A. Orszag, Advanced Mathematical Methods for Scientists and Engineers, McGraw-Hill, New York, 1978.
[64] W. van Saarloos, P.C. Hohenberg, Fronts, pulses, sources and sinks in generalized complex Ginzburg–Landau equations, Physica D 56 (1992) 303–367.